

Physics-informed Machine Learning-based Methodology for Plated Through Holes Lifetime Estimation in Printed Circuit Boards

Marco Sperti¹, Chinmay Nawghane¹, Bart Vandeveld¹, Nicolas Lammens², Mathias Verbeke^{3,4}

¹imec, Leuven, Belgium

²Siemens Industry Software nv, Strategy & Innovation, Leuven, Belgium

³Department of Computer Science, KU Leuven, Belgium

⁴Flanders Make@KU Leuven, Belgium

Marco.Sperti@imec.be

Abstract—The increasing demand for reliable electronics underscores the need for predictive tools to estimate component lifetimes and mitigate key failure risks and associated costs. This study focuses on Plated Through Holes (PTHs) in Printed Circuit Boards, which are critical to system reliability but prone to failures under standard thermal cycling due to strain from coefficient of thermal expansion mismatches. A physics-informed machine learning-based methodology is proposed, integrating data from Finite Element Method simulations and experimental data from degradation tests. Two machine learning models are combined to estimate the Remaining Useful Life of PTHs: a feedforward neural network (FFNN) able to predict the number of cycles to failure of a given structure and trained on a Design of Experiment dataset with geometric and material parameters, and a Long Short-Term Memory (LSTM) network to predict the temporal degradation trend measured by real sensors on the board. The combination of these two models allows the implementation of a Physics-informed Neural Network where the physics learned based on the FFNN is used as a physical constraint in the cost function of the LSTM to guide the prediction of the degradation.

Keywords—Printed circuit boards, plated through holes, data-driven approach, degradation, physics-informed neural network

I. INTRODUCTION

The increasing complexity and miniaturization of electronic systems have amplified the importance of ensuring their reliability. Failures in critical components can lead to significant economic losses and operational disruptions, especially in sectors such as aerospace, automotive, and telecommunications. Among the key reliability challenges in these systems are Printed Circuit Boards (PCBs), which serve as the backbone for electronic interconnections. Within PCBs, Plated Through Holes (PTHs) play a vital role in establishing electrical connections between layers, but their susceptibility to thermal and mechanical stresses makes them a common failure point. PTH failures are often induced by cyclic thermal loading, which arises due to the mismatch in the Coefficient of Thermal Expansion (CTE) between the copper plating and the surrounding composite material. This mismatch generates localized strains leading to crack initiation and propagation

through the copper layer. Such failures compromise the electrical integrity of the system and are a major concern for PCB manufacturers and end-users. Experimental studies and Finite Element Method (FEM) simulations have extensively investigated these phenomena, highlighting the importance of accurate lifetime prediction models for PTHs [1]–[5]. Traditional preventive maintenance relies on fixed schedules for inspections and component replacements. While this approach minimizes the risk of unexpected failures, it often results in unnecessary interventions and increased costs. Predictive maintenance (PdM), on the other hand, leverages real-time condition monitoring and advanced analytical models to estimate the Remaining Useful Lifetime (RUL) of components, enabling timely interventions that optimize resource utilization and system reliability [6], [7]. By employing predictive maintenance, systems can reduce downtime, avoid catastrophic failures, and enhance operational efficiency. For example, time series prediction algorithms and neural network-based methods have been used to predict degradation trajectories and preemptively address failures, showcasing the advantages of PdM over traditional strategies [7]. Two primary methodologies dominate the field of RUL estimation: physics-based models and data-driven models. Physics-based models rely on fundamental principles to describe material behavior under cyclic loading [4], [5]. These models provide interpretability and reliability but often require extensive calibration and computational resources. Conversely, data-driven approaches leverage sensor data and machine learning (ML) algorithms to predict failures based on historical and real-time data.

Machine learning has become a cornerstone of data-driven RUL estimation, with algorithms like Long Short-Term Memory (LSTM) networks demonstrating remarkable success in capturing temporal dependencies in sensor data. LSTMs are particularly effective in modeling degradation patterns and predicting RUL, as they can process sequential data while mitigating issues of vanishing gradients common in traditional recurrent neural networks [8], [9].

However, challenges such as data scarcity, overfitting, and the black-box nature of ML models remain significant hurdles.

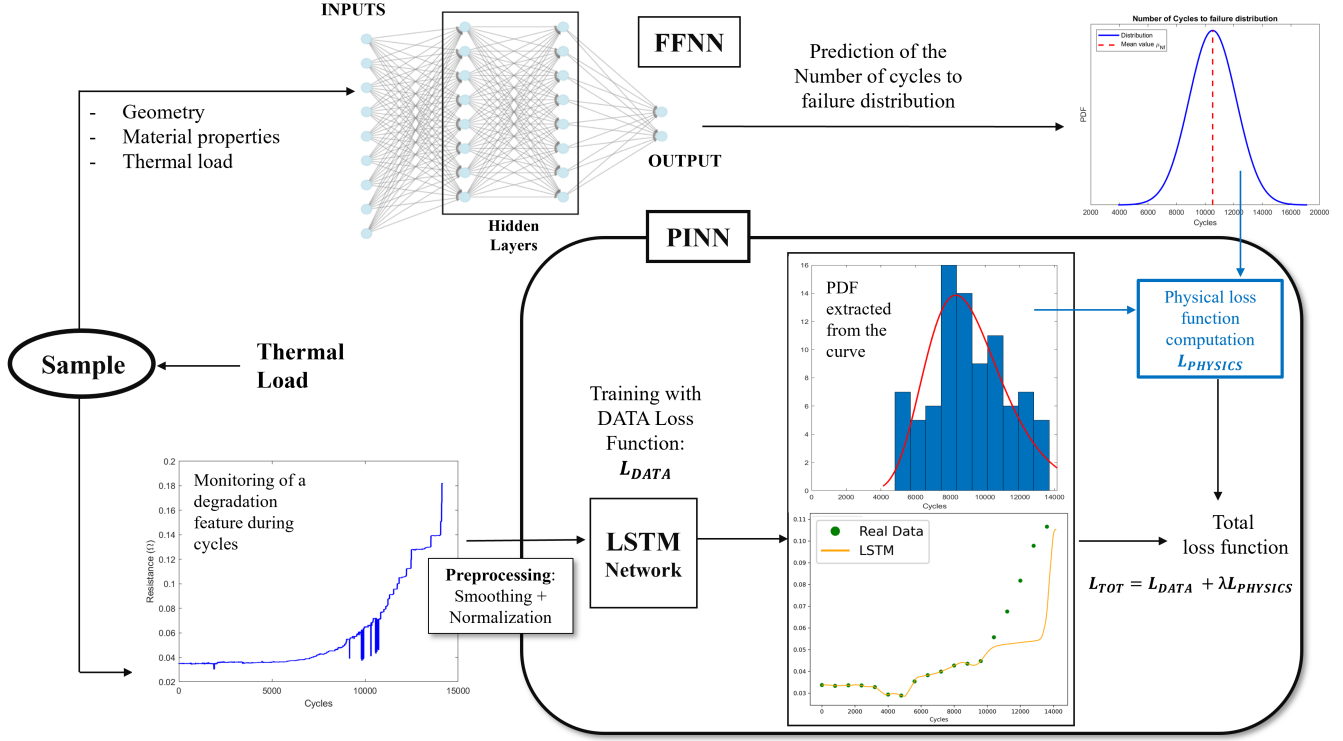


Fig. 1. Workflow of the proposed model for lifetime prediction of PTHs. The diagram illustrates the data flow and the integration of the Machine Learning techniques used. Starting from a sample subjected to thermal load, the model follows two distinct branches. (a) Upper branch: a Feedforward Neural Network (FFNN) predicts the Number of cycles to failure based on data from FEM simulations and on the knowledge of the input features (geometry, material properties, thermal load). (b) Lower branch: an LSTM is trained on an experimental degradation dataset to predict the resistance evolution over time. The PINN framework integrates both predictions by combining data-driven loss and physics-based loss.

Integrating domain knowledge, such as using PINNs, has proven effective in enhancing both the accuracy and interpretability of predictions [7], [10]. While data-driven models excel in handling large datasets and capturing complex interactions, they may lack physical interpretability and robustness when extrapolating beyond the training data [6], [11]. Hybrid models, such as Physics-Informed Neural Networks (PINNs), aim to bridge this gap by embedding physical laws into the cost functions of data-driven models, ensuring predictions remain consistent with known physics [11].

This study builds on these advancements by proposing a novel physics-informed machine-learning methodology to estimate the RUL of PTHs subjected to thermal cycling. The approach integrates FEM simulations to model strain distributions and experimental data from PCB test boards. ML models are trained on these datasets to predict strain amplitude and degradation trends, offering a scalable and efficient solution for predictive maintenance in electronic systems. The novelty of this approach lies in the integration of data from FEM simulations and experimental measurements, allowing the models to leverage both synthetic and real-world degradation patterns. This hybrid methodology enhances predictive accuracy by ensuring that the learned features incorporate both physics-based constraints and observed degradation behavior.

II. RELATED WORK

The application of data-driven methodologies and physics-informed approaches in reliability assessment has been widely explored in the literature. However, their combination, particularly in the context of electronics prognostics, remains a relatively unexplored field. In this section, we provide an overview of existing approaches, first discussing data-driven methods for reliability assessment and then reviewing physics-informed methodologies for prognostics. Finally, we highlight how our proposed method uniquely integrates real-world sensor data with physics-based simulations within a PINN, improving robustness and prediction accuracy.

A. Data-Driven approaches

In recent years, the application of ML and Deep Learning (DL) in electronics prognostics has gained significant attention. Various studies have explored data-driven methodologies to estimate the RUL of electronic components and systems, leveraging ML techniques to enhance predictive accuracy. These approaches often complement or replace traditional physics-based models, offering scalable and adaptive solutions for reliability assessment. Bhat et al. provide a comprehensive review on the application of machine learning algorithms in prognostics and health monitoring (PHM) of electronic

systems, highlighting key challenges and advancements in data-driven reliability assessment [12]. Ferrando-Villalba and Vandeveld developed an Artificial Neural Network (ANN) regressor to predict inelastic strain in PBGA solder joints under thermal cycling, demonstrating that ML models can significantly reduce computational costs compared to traditional FEM simulations while maintaining an acceptable prediction accuracy [13]. Yao et al. proposed a physics-based nested ANN approach to predict the reliability of Fan-Out Wafer-Level Packages (FOWLP), integrating material property estimation and mechanical response prediction to improve accuracy and computational efficiency [14]. Chou and Chiang developed an ANN regression model to assess the long-term reliability of wafer-level packages (WLPs), leveraging FEM simulations combined with empirical mechanics theories to predict solder joint fatigue life efficiently [15]. Alghassi et al. developed a computationally efficient and embeddable prognostic approach for power electronics, leveraging a data-driven method to predict the RUL of insulated-gate bipolar transistors (IGBTs) based on accelerated aging experiments and stochastic degradation modeling [16].

B. Physics-Informed approaches

Beyond data-driven strategies, physics-based models provide an alternative means of predicting system degradation by leveraging fundamental material properties and failure mechanisms. These approaches, such as finite element simulations and empirical fatigue models, offer high interpretability and generalizability but often require extensive calibration and computational resources. Zheng et al. proposed a LSTM network for RUL estimation, demonstrating its effectiveness in capturing sequential dependencies in sensor data and outperforming traditional regression-based methods and Convolutional Neural Networks (CNNs) in prognostics applications [17]. Meszmer et al. explored the use of deep neural networks for stress prognostics in encapsulated electronic packages, demonstrating that LSTM and GRU architectures effectively predict stress distribution and degradation patterns based on time-series data from in-situ condition monitoring during thermal shock tests [18]. Zhang et al. proposed a LSTM Recurrent Neural Network (RNN) for predicting the RUL of lithium-ion batteries, demonstrating its ability to capture long-term dependencies in battery degradation data and improve prediction accuracy compared to traditional machine learning methods [19]. Habibollahi Najaf Abadi and Modarres introduced a guided neural network framework for predicting system degradation, integrating a physics discovery neural network with a predictive model to enhance the accuracy and robustness of lifetime estimation in engineering systems [11]. Wen et al. introduced a PINN framework for PHM of lithium-ion batteries, integrating empirical and physics-based models to improve RUL estimation accuracy and model generalizability [20]. Li et al. introduced a PINN approach for compact device modeling, incorporating fundamental device physics into neural network architectures to ensure physically consistent and computationally efficient predictions [21]. Habibollahi

Najaf Abadi and Modarres proposed a deep learning framework for discovering the underlying physics of degradation in data-driven prognostics, integrating a predictive model with a physics discovery network to improve interpretability and generalization in RUL estimation [22].

The methodology proposed in this paper bridges the gap between these two paradigms by integrating data from real-world sensor measurements and finite element simulations within a PINN. Unlike previous studies that rely exclusively on either experimental degradation data or physics-based simulations, our approach leverages both, ensuring a more robust and generalizable prediction model. By embedding physics constraints directly into the learning process, we enhance the model's ability to extrapolate beyond the training dataset while maintaining consistency with established failure mechanisms. This hybrid methodology significantly improves predictive accuracy in PCB reliability assessment, offering a scalable and interpretable solution for PTH lifetime estimation.

III. BACKGROUND

Plated Through Holes are critical interconnect structures in PCBs, ensuring electrical continuity between different layers and different components of the circuit. However, their reliability is challenged by thermomechanical stresses induced by CTE mismatches between the copper plating and the surrounding composite material (typically FR4). These strains accumulate over repeated thermal cycles, leading to material fatigue and eventual failure [1].

A. Failure Mechanisms in PTHs

PTH failures predominantly originate from low-cycle fatigue (LCF), where cyclic plastic deformation induces crack initiation and propagation within the electroplated copper walls [2]. The primary causes of these failures include:

- *CTE mismatch-induced strain*: Due to thermal cycling (e.g., between -50°C and 125°C in automotive applications [23]), the copper expands and contracts at a different rate compared to the PCB laminate. This results in localized plastic deformation, particularly at stress concentration points (e.g., knee regions of the PTH) [3].
- *Microstructural defects*: Electroplated copper in PTHs exhibits grain boundary weaknesses and residual stresses from the deposition process. These factors accelerate fatigue failure by promoting crack nucleation and void formation [5]. This effect is not considered in the model.

To predict the RUL of PTHs, classical fatigue models are employed, primarily the Coffin-Manson equation [2] and the Paris law [24], [25] for crack propagation.

The fatigue life N_f of a given structure can be estimated using the Coffin-Manson relationship:

$$\Delta\varepsilon = \frac{\sigma'}{E} (2N_f)^b + \varepsilon' (2N_f)^c \quad (1)$$

where $\Delta\varepsilon$ is the strain amplitude defined as the difference of the strain accumulated at the extreme points of the applied thermal load. It is defined as the sum of an elastic and a plastic

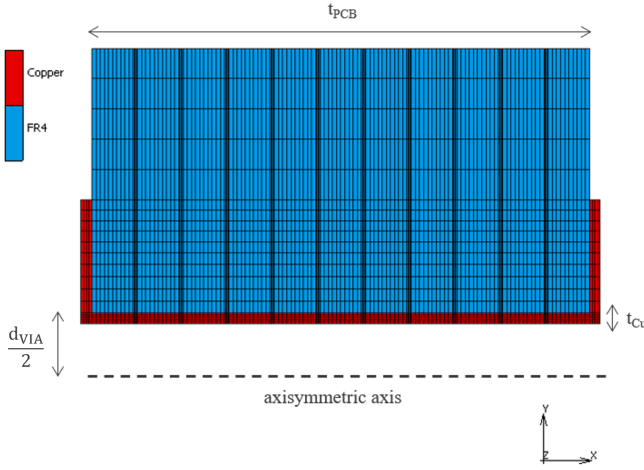


Fig. 2. Axisymmetric model of the PTH for the FEM simulation.

term. In Eq. 1, b and c are respectively the elastic and plastic exponents, σ'/E is called the cyclic resistance coefficient, and ϵ' is the fatigue ductility coefficient.

Cracks propagate following Paris' law (Eq. 2), which describes the crack growth rate $\frac{da}{dN}$ as a function of the stress intensity factor range ΔK :

$$\frac{da}{dN} = A(\Delta K)^m \quad (2)$$

where A and m are empirical constants dependent on the material microstructure [26]. This phase is crucial for understanding the time to final failure cycle once a crack has initiated. Finite Element Analysis (FEA) and experimental thermal cycling tests validate these fatigue models by correlating strain distributions with observed crack initiation and propagation locations [2]. Studies confirm that reducing PTH aspect ratio, increasing copper plating thickness, and optimizing PCB material selection can significantly enhance fatigue life [3].

B. Machine Learning techniques for fatigue life prediction

Machine Learning techniques have gained increasing relevance in fatigue life prediction by capturing complex stress-strain relationships and estimating the fatigue life N_f of critical electronic components. This paragraph provides an overview of the Feedforward Neural Networks, Long Short-Term Memory networks, and Physics-Informed Neural Networks, which are leveraged in the methodological approach proposed in this paper.

- A Feedforward Neural Network (FFNN) is one of the simplest architectures in deep learning, where information flows only in one direction, from the input layer to the output layer, through one or more hidden layers. Each neuron processes a weighted sum of the inputs, followed by a non-linear activation function (σ in Eq. 3). The mathematical formulation is:

$$h^{(l)} = \sigma \left(W^{(l)} h^{(l-1)} + b^{(l)} \right) \quad (3)$$

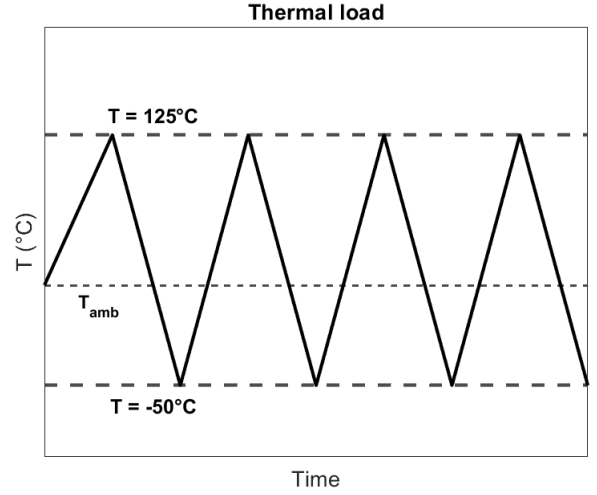


Fig. 3. Applied thermal load

where $h^{(l)}$ and $h^{(l-1)}$ are respectively the output and the input of the layer l , $W^{(l)}$ is the weight matrix, and $b^{(l)}$ is the bias vector [27], [28]. The aim of this network, depicted in the upper branch in Fig. 1, is the lifetime prediction for a given unseen input pattern, concerning the geometry, material properties, and thermal loads.

- Unlike FFNNs, which do not capture temporal dependencies, Long Short-Term Memory (LSTM) networks, whose unit cell is depicted as a type of Recurrent Neural Network (RNN) specifically designed to model sequential data. This makes LSTMs particularly effective for fatigue crack growth prediction, where past loading conditions influence future damage accumulation [8], [9].
- While conventional ML models like FFNN and LSTMs rely purely on data, Physics-Informed Neural Networks (PINN) incorporate physical knowledge (e.g. partial differential equations) into the learning process, ensuring that predictions remain consistent with the physics of the problem (the degradation process due to strain accumulation in this study). The loss function of the PINN in Eq. 4 is composed of two terms:

$$L = L_{\text{data}} + \lambda L_{\text{physics}} \quad (4)$$

where L_{data} represents the traditional data loss (e.g., Mean Squared Error), L_{physics} enforces physical consistency, and λ is a weighting factor that balances the two terms [21], [22].

IV. METHODOLOGY

The aim of this work is to develop a methodology to predict the remaining useful lifetime with a more robust model, through the combination of two different types of data described in the following paragraphs.

A. Data from FEM simulations

Finite Element Method (FEM) is widely used to model the behaviour of structures made by different materials and

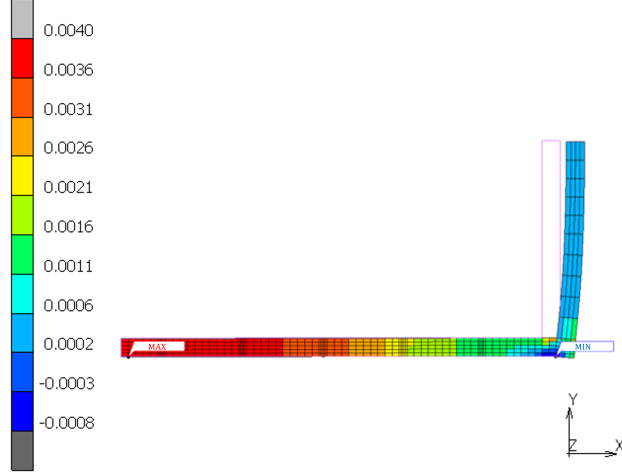


Fig. 4. Axial strain distribution at $T = 125^\circ\text{C}$ in the copper layer

subjected to thermal loads to estimate the stress and strain distribution. Due to the rotational symmetry of the structure, an axisymmetric model has been implemented to reduce the computational time compared to a 3D one, as shown in Fig. 2, following the approach proposed in [29]. The materials involved are: Copper, modeled as elastic-plastic isotropic; FR4, the composite material of the board, treated as elastic-plastic orthotropic material, and so, its material properties are represented by a tensor. Since the model is 2D, the mesh is made by 4-noded elements and it has been made finer at the interface between the two materials where more accuracy is needed in the calculation of stress and strain. Due to the symmetry along the X direction, only half of the structure was retained to further increase the simulation speed. The thermal profile in Fig. 3 is applied to the structure and the strain distribution is evaluated at its extreme points: -50°C and 125°C . Fig. 4 shows the strain distribution in the Copper layer at $T = 125^\circ\text{C}$ and the volume with the maximum values, the damage volume, is the one in the middle. The same happens at the lower temperature. So, the average strain is extracted from these elements of the mesh and the strain amplitude is evaluated with the formula:

$$\Delta\varepsilon = \varepsilon_{\text{avg}}(T = 125^\circ\text{C}) - \varepsilon_{\text{avg}}(T = -50^\circ\text{C}) \quad (5)$$

so that Eq. 1, the Coffin-Manson model, can be used to evaluate the Number of Cycles to Failure.

To prepare a training dataset for the ML-based approach, a Design of Experiments has been built by selecting some features described in Table 1 and by using the Latin hypercube sampling method [30], [31]. The resulting dataset has 10.000 samples with different geometry, material properties and ther-

mal loads, and consequently also different $\Delta\varepsilon$ computed as in Eq. 5.

TABLE I
DESIGN OF EXPERIMENTS. FEATURES AND RANGES

Feature	Min	Max
d_{VIA} (mm)	0.25	0.6
t_{PCB} (mm)	1.0	2.5
t_{Cu} (μm)	25	40
$E_{\text{FR4},z}$ (GPa)	4	10
$\text{CTE}_{\text{FR4},z}$ ($\text{ppm}/^\circ\text{C}$)	50	70
Y_{Cu} (MPa)	150	250
T_{min} ($^\circ\text{C}$)	-55	0
T_{max} ($^\circ\text{C}$)	85	150

The strain amplitude has been converted into Number of Cycles to Failure through the Coffin-Manson model previously optimized and therefore now the regression task no longer only involves the prediction of a real number, but of a distribution, and therefore of mean value and standard deviation.

B. Data from experimental test

Experimental data were collected from PCB boards containing 12 arrays of PTHs (10×10 arrays, 100 PTHs per array). Each array has a distinct geometric configuration (innerland configuration and diameter). The schematic of the board is depicted in Fig. 5a and 5b. During testing, electrical resistance of each array is monitored under thermal cycling. Resistance increases indicate failure in one or more PTHs in the array. These data (i.e. the resistance measurements for the arrays with Configuration A are reported in Fig. 5c) are used to train an LSTM model that predicts resistance evolution over cycles, allowing the estimation of N_f . To obtain the N_f from these curves, a parametric model has been created for the equivalent resistance of a single array with the following assumptions:

- All the PTHs in an array are independent. Validation of this hypothesis has been obtained through FEM simulation of a 3D array.
- The zoom in Fig. 5c shows that, apart from noise, the increase in resistance value occurs via steps. For the model it was assumed that each single resistance, when failure occurs at a certain N_f , increases as a stepwise function: The stepwise function:

$$R_{\text{PTH},i}(N) = \begin{cases} R_{\text{init}}, & N < N_f \\ \infty, & N \geq N_f \end{cases} \quad (6)$$

where N represents the cycles.

The index i in Eq. 6 runs from 1 to 100 and represents the single PTH within an array.

The equivalent resistance of an array can be expressed as:

$$R_{\text{eq}}(N) = R_s + \left(\frac{1}{\sum_{i=1}^{100} \frac{1}{R_{\text{PTH},i}(N)}} \right) \quad (7)$$

where R_s is a series resistance connected to the array. The corresponding model is shown in Fig. 6a. $R_{\text{eq}}(N)$ depends

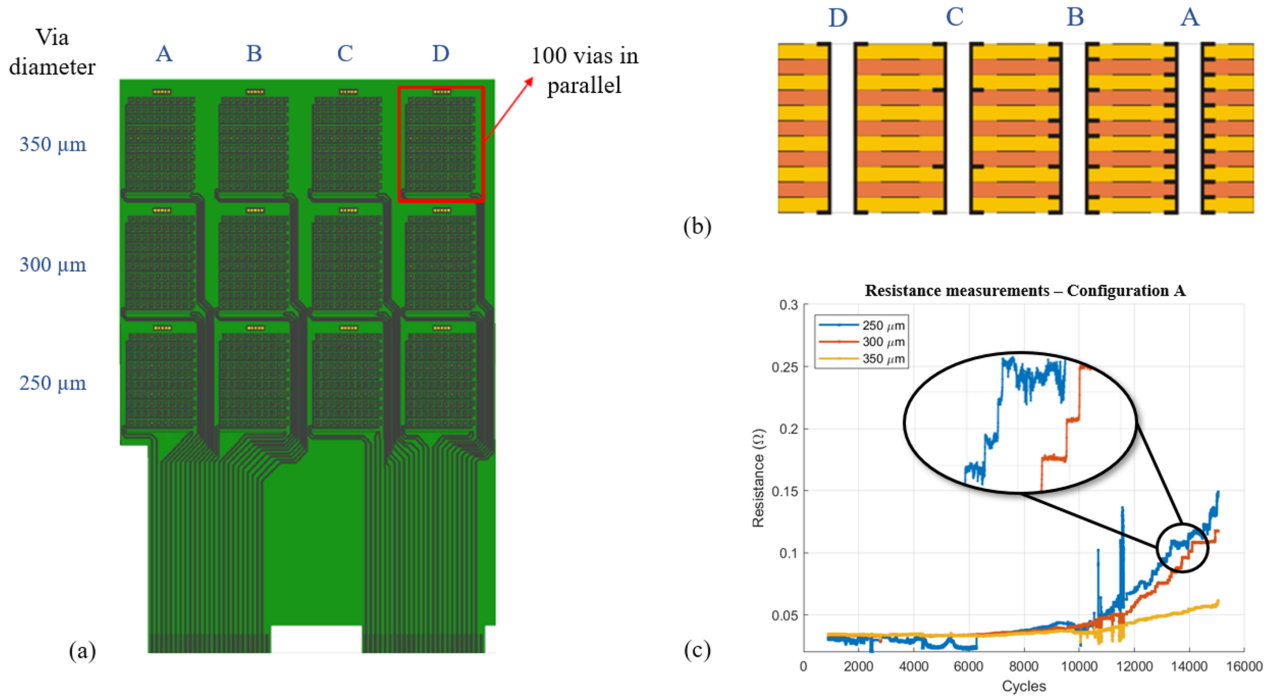


Fig. 5. (a) Schematic of the board used for experimental tests: measurements are made on 12 arrays of 100 PTHs connected in parallel and each array is characterized by a geometric configuration (b) Schematic of the configuration of the non-functional copper pads (or innerlands) within the thickness of the PCB. (c) Resistance measurements of the PTH arrays with configuration A

on 100 values of N_f that must be optimized to fit the curve of the model with the experimental ones. The result of this fitting (Fig. 6b) provides a distribution of the N_f for a given array (and so, for a given geometrical configuration) in terms of mean values and standard deviation. Eq. 2 has been used to compute the number of cycles from the crack initiation to the end of the crack propagation as explained in [32], [33] and these distributions of the N_f are used to tune the empirical parameters of the Coffin-Manson model (Eq. 1) to compute the N_f in terms of mean value and standard deviation starting from the predicted $\Delta\varepsilon$.

Some preprocessing is needed before the training process to improve the prediction performances: (a) The Moving Average filtering method [34] with 5% window size was applied to smooth the curves and remove noise and spikes from the measurements and (b) A scaling as described in Eq. 8 and 9 was performed to normalize the curves so that they all start at 100%, with their values decreasing as the number of applied cycles increases.

$$R_{\text{norm},k}(N) = \frac{R_k(N) - R_k(N=0)}{R_{\text{max},k} - R_k(N=0)} \quad (8)$$

$$SoH_k(N) = 100 \cdot [1 - R_{\text{norm},k}(N)] \quad (9)$$

where the index k runs from 1 to 12 and represents the array. $R_k(N)$ is the time evolution of the resistance of array k , $R_k(N=0)$ and $R_{\text{max},k}$ are the initial and maximum values of the resistance of array k .

The transformation allows the resistance values to be converted into the overall State of Health (SoH) [19], [20] of the entire array.

C. Lifetime prediction

Through this analysis the two different types of data are consistent to build the PINN including the physical knowledge in the first FFNN into the loss function of the LSTM and to have a guided prediction of the resistance increase as a function of the applied cycles.

It is important to remark the fact that the output of the LSTM is the value of the resistance at the next cycle, and so it is able to predict the entire resistance curve $R_{k,\text{pred}}(N)$. Thanks to the fitting strategy described to obtain the distribution of the number of cycles to failure, it is possible to associate a distribution $N_{f,\text{pred}}$ to the predicted curve. These two outputs are shown in the lower branch in Fig. 1.

$$L_{\text{physics}} = \|N_{f,\text{physics}} - N_{f,\text{pred}}\| \quad (10)$$

$$L_{\text{data}} = \sum_{N=1}^{N^{\text{EXP}}} [R_k(N) - R_{k,\text{pred}}(N)]^2 \quad (11)$$

If the geometric and mechanical parameters of the structure under measurement, as listed in Table I, are known, the FFNN can be used to predict the N_f distribution. This distribution acts as the physical constraint ($N_{f,\text{physics}}$), as it is derived

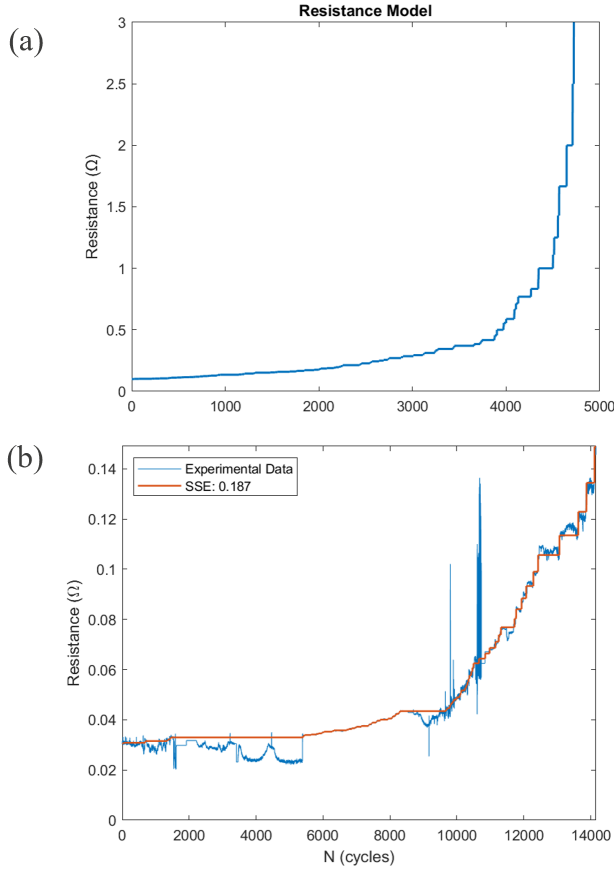


Fig. 6. (a) Model of the equivalent resistance of a single array on the board, described by Eq. 6 and 7. (b) Fitting between the model and experimental curve

from a neural network trained on a dataset generated through FEM simulations, ensuring that it inherently incorporates the physics of the problem. Thus, during each epoch, the PINN training process is carried out by computing the loss function, using Eq. 4 as the sum of: (a) a data-based term, which is the MSE between the real and predicted resistance curves (Eq. 11) and (b) a physics-based term in Eq. 10, which evaluates the difference between the predicted and physical N_f distributions.

Eq. 10 describes the physical constraint. The distance between two distributions can be measured as MSE or, with a more rigorous approach, through the Kullback-Leibler divergence criteria [35]. This method has been implemented in the framework described in this paper.

V. EXPERIMENTS AND RESULTS

In this section the application and results of the three models described in Fig. 1, the FFNN, the LSTM and the PINN, will be shown and discussed. The aim is to demonstrate that the integration of the predictions made by the FFNN trained on the FEM data improves the prediction of the trend of the electrical resistance along the applied thermal cycles.

- The FFNN has been trained with 80% of the dataset and tested with the remaining 20%. The architecture is composed by 2 hidden layers with 64 neurons and ReLU activation function. The architectural selection has been done by selecting the one with the smallest error on the validation set, randomly extracting 20% samples from the training set. The two outputs represent the mean value and the standard deviation of N_f . A softplus activation is added to the standard deviation output neuron to impose it to be positive, while a linear one is used for the mean value. The prediction capability of this FFNN can be observed in the scatter plot in Fig. 7.
- To train the LSTM the dataset was divided into three subsets for training, validation, and testing. Specifically, 8 time series (approximately 70% of the total 12 resistance measurements) were used for training, while 2 time series were allocated for validation, and the remaining 2 series were assigned to the test set. The split was performed randomly to ensure a balanced distribution of data across the three phases.

For each time series, a sliding time window containing N resistance values was defined. The LSTM model was trained to predict the next resistance value based on the first $N-1$ values within the window. The parameter N directly impacts both the training time and the model's computational complexity: larger window sizes allow for capturing long-term temporal dependencies more effectively but also increase computational cost and the risk of overfitting. A window size of $N=5$ yielded good results, even in terms of predictions on the test set.

Since LSTM is a deep learning approach, it is crucial to minimize overfitting and to improve the generalization performance of the predicted output.

Various regularization techniques were tested, and the

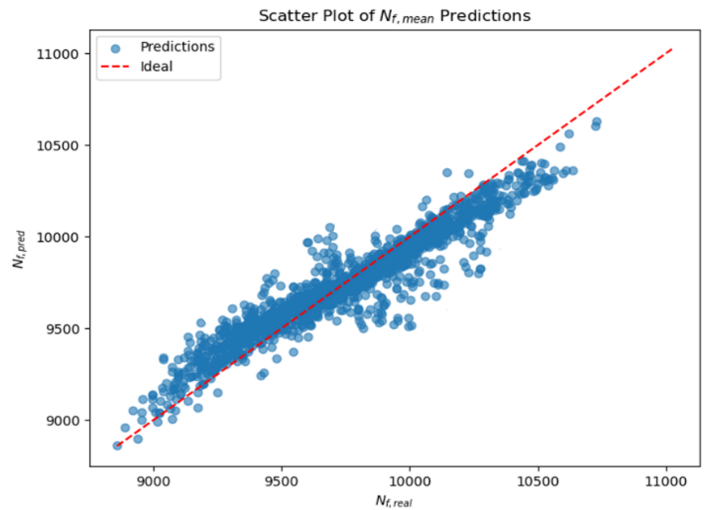
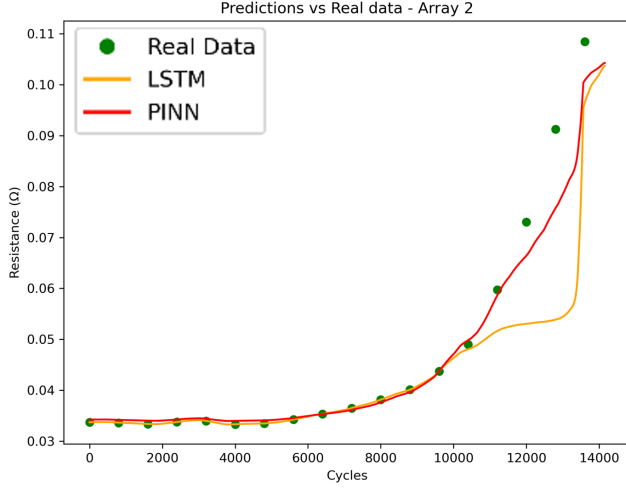
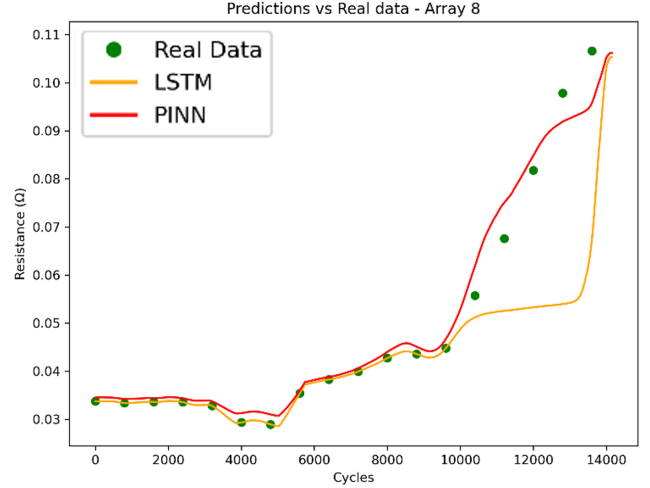


Fig. 7. Predicted vs Real number of cycles to failure of the samples in the test set for the FFNN regressor



(a)



(b)

Fig. 8. Time series prediction. Comparison between LSTM and PINN approaches for the resistance curves in the test set, corresponding to the second and eighth arrays on the board: (a) Configuration A, $d = 300 \mu\text{m}$ and (b) Configuration C, $d = 300 \mu\text{m}$

most effective one was found to be Dropout at 30%, as it resulted in the model that minimized the validation loss. The results for the array 2, which belong to the test set, are summarized in Table II.

TABLE II
LSTM RESULTS, ARRAY 2

Regularization	Prediction Error
NO	31.141
30% dropout	17.953

MSE was used to compute these metrics. Without regularization, the network overfits by memorizing patterns and noise, leading to poor generalization. Dropout mitigates this by randomly deactivating neurons, forcing the model to learn more robust representations. While this decreases accuracy on the training set, it improves performance on unseen data, as shown by the lower test error.

TABLE III
PREDICTION ERROR COMPARISON, TEST SET

Array	LSTM	PINN
2	17.953	6.562
8	19.924	8.054

- Once the two architectures have been trained and optimized to make predictions on their respective data types, the PINN can be constructed as explained in Section IV and illustrated in Fig. 1.

The λ parameter in Eq. 4 has been set to 0.1.

This approach ensures that the model remains consistent with the underlying physical principles while leveraging

data-driven learning for enhanced predictive accuracy. The prediction error for the trend of the resistance corresponding to arrays in the test set, computed with Eq. 11, between the predicted curve with PINN approach and the real curve are reported in Table III, resulting in an improvement of the prediction performances of approximately 63% for array 2 and 59% for array 8.

Fig. 8a and 8b present a comparison between the two approaches, demonstrating how incorporating the physics of the problem leads to improved prediction performance, particularly in the most relevant section for failure prediction, where the resistance increases. The plots show the results for Array 2 and 8 of the board.

Integrating the physics of the problem into the loss function to be minimized significantly enhances the accuracy of resistance trend prediction. Previously, the LSTM model relied solely on data, leading to potential overfitting and limited generalization when applied to unseen configurations.

By incorporating physics-based constraints through the PINN framework, the model is guided towards physically consistent predictions, reducing error and improving robustness. The comparative analysis, summarized in Table III, demonstrates that across all tested arrays, the PINN approach consistently achieves lower prediction errors than the purely data-driven LSTM model.

To obtain more reliable and robust results, the model was trained and validated using different configurations of the three sets (training, validation, and test), consistently yielding similar results to those reported.

VI. CONCLUSION

In this work, we demonstrated that implementing a Physics-Informed Neural Network (PINN) for predicting the degradation over time of Plated Through Holes (PTHs) significantly improves performance compared to a purely data-driven approach. Given that PTHs are critical components present in all PCBs, and that they can also be used as canary sensor in electronic systems, understanding their degradation behaviour is essential. A key aspect of our approach is that, despite incorporating physics-based constraints, it remains almost entirely data-driven. Unlike traditional PINNs, we do not include differential equations in the loss function. The only physical constraint applied is the boundary condition from the FEM simulations. As a result, we successfully trained a neural network that accurately predicts degradation states using a very limited degradation dataset (only 12 signals). Moreover, constructing the physics-based dataset did not require designing and executing a long-term experimental campaign, which is often a major bottleneck in this field. Instead, our Design of Experiments (DoE) approach enabled us to obtain strain amplitude data for 10.000 samples across different configurations in just four days. This effectively addresses a well-known issue in the literature (the lack of degradation data) while significantly reducing time and resource constraints. These results highlight the potential of combining physics-informed and data-driven methodologies to enhance the predictive capabilities of reliability models for electronic components, paving the way for more efficient and scalable prognostic solutions in PCB health monitoring.

ACKNOWLEDGMENT

This research was conducted within the MIRELAI project, Funded by the European Union (Grant Agreement No. 101072491). Views and opinions expressed are however those of the author(s) only and do not necessarily reflect those of the European Union or the European Research Executive Agency. Neither the European Union nor the granting authority can be held responsible for them.

REFERENCES

- [1] K. Weinberg and W. H. Müller, "A strategy for damage assessment of thermally stressed copper vias in microelectronic printed circuit boards," *Microelectronics Reliability*, vol. 48, no. 1, pp. 68–82, 2008.
- [2] F. Su, R. Mao, J. Xiong, K. Zhou, Z. Zhang, J. Shao, and C. Xie, "On thermo-mechanical reliability of plated-through-hole (pth)," *Microelectronics Reliability*, vol. 52, no. 6, pp. 1189–1196, 2012.
- [3] A. Salahouelhadj, M. Martiny, S. Mercier, L. Bodin, D. Manteigas, and B. Stephan, "Reliability of thermally stressed rigid–flex printed circuit boards for high density interconnect applications," *Microelectronics Reliability*, vol. 54, no. 1, pp. 204–213, 2014.
- [4] K. Fellner, T. Antretter, P. F. Fuchs, and Q. Tao, "Numerical simulation of the electrical performance of printed circuit boards under cyclic thermal loads," *Microelectronics Reliability*, vol. 62, pp. 148–155, 2016.
- [5] K. Watanabe, Y. Kariya, N. Yajima, K. Obinata, Y. Hiroshima, S. Kikuchi, A. Matsui, and H. Shimizu, "Low-cycle fatigue testing and thermal fatigue life prediction of electroplated copper thin film for through hole via," *Microelectronics Reliability*, vol. 82, pp. 20–27, 2018.
- [6] H. H. N. Abadi and M. Modarres, "A deep learning approach for discovering the underlying physics of degradation for data-driven prognostics," in *Annual Reliability and Maintainability Symposium (RAMS)*, 2024, pp. 20–24.
- [7] C.-Y. Lin, Y.-M. Hsieh, F.-T. Cheng, H.-C. Huang, and M. Adnan, "Time series prediction algorithm for intelligent predictive maintenance," *IEEE Robotics and Automation Letters*, vol. 4, no. 3, pp. 2807–2814, 2019.
- [8] S. Zheng, K. Ristovski, A. Farahat, and C. Gupta, "Long short-term memory network for remaining useful life estimation," in *IEEE International Conference on Prognostics and Health Management (ICPHM)*, 2017.
- [9] Y. Zhang, R. Xiong, H. He, and M. G. Pecht, "Long short-term memory recurrent neural network for remaining useful life prediction of lithium-ion batteries," *IEEE Transactions on Vehicular Technology*, vol. 67, no. 7, pp. 5695–5705, 2018.
- [10] M. S. Haque, M. N. B. Shaheed, and S. Choi, "Rul estimation of power semiconductor switch using evolutionary time series prediction," in *IEEE International Symposium on Industrial Electronics (ISIE)*, 2018.
- [11] H. H. N. Abadi and M. Modarres, "Predicting system degradation with a guided neural network approach," *Sensors*, vol. 23, p. 6346, 2023.
- [12] D. Bhat, S. Muench, and M. Roellig, "Application of machine learning algorithms in prognostics and health monitoring of electronic systems: A review," *e-Prime - Advances in Electrical Engineering, Electronics and Energy*, vol. 4, p. 100166, 2023.
- [13] P. Ferrando-Villalba and B. Vandevelde, "Bga solder strain prediction using an artificial neural network regressor," in *2022 23rd International Conference on Thermal, Mechanical and Multi-Physics Simulation and Experiments in Microelectronics and Microsystems (EuroSimE)*, 2022.
- [14] P. Yao, J. Yang, Y. Zhang, X. Fan, H. Chen, J. Yang, and J. Wu, "Physics-based nested-ann approach for fan-out wafer-level package reliability prediction," in *2022 IEEE 72nd Electronic*, 2022.
- [15] P. H. Chou and K. N. Chiang, "Reliability assessment of wafer level package using artificial neural network regression model," *Journal of Mechanics*, vol. 35, no. 6, pp. 829–837, Dec. 2019.
- [16] A. Alghassi, S. Perinpanayagam, M. Samie, and T. Sreenuch, "Computationally efficient, real-time, and embeddable prognostic techniques for power electronics," *IEEE Transactions on Power Electronics*, vol. 30, no. 5, pp. 2623–2634, May 2015.
- [17] S. Zheng, K. Ristovski, A. Farahat, and C. Gupta, "Long short-term memory network for remaining useful life estimation," in *2017 IEEE International Conference on Prognostics and Health Management (ICPHM)*, 2017.
- [18] P. Meszmer, M. Majd, A. Prisacaru, P. J. Gromala, and B. Wunderle, "Neural networks for enhanced stress prognostics for encapsulated electronic packages - a comparison," *Microelectronics Reliability*, vol. 123, p. 114181, 2021.
- [19] Y. Zhang, R. Xiong, H. He, and M. G. Pecht, "Long short-term memory recurrent neural network for remaining useful life prediction of lithium-ion batteries," *IEEE Transactions on Vehicular Technology*, vol. 67, no. 7, pp. 5695–5705, July 2018.
- [20] P. Wen, Z.-S. Ye, Y. Li, S. Chen, P. Xie, and S. Zhao, "Physics-informed neural networks for prognostics and health management of lithium-ion batteries," *IEEE Transactions on Intelligent Vehicles*, vol. 9, no. 1, pp. 2276–2288, Jan. 2024.
- [21] M. Li, O. Irsoy, C. Cardie, and H. G. Xing, "Physics-inspired neural networks for efficient device compact modeling," *IEEE Journal on Exploratory Solid-State Computational Devices and Circuits*, vol. 2, pp. 44–49, Dec. 2016.
- [22] H. H. N. Abadi and M. Modarres, "A deep learning approach for discovering the underlying physics of degradation for data-driven prognostics," in *2024 Annual Reliability and Maintainability Symposium (RAMS)*, 2024.
- [23] J. Gao and J. B. Kwak, "Reliability and thermal fatigue life prediction of solder joints for advanced automotive microelectronics," *Journal of Mechanical Science and Technology*, vol. 35, no. 8, pp. 3633–3641, 2021.
- [24] P. Miarka, S. Seitzl, V. Bílek, and H. Cifuentes, "Assessment of fatigue resistance of concrete: S-n curves to the paris' law curves," *Construction and Building Materials*, vol. 341, p. 127811, 2022.
- [25] G. Joshi and S. Mall, "Crack initiation and growth from pre-corroded pits in aluminum 7075-t6 under laboratory air and salt water environments," *Journal of Materials Engineering and Performance*, vol. 26, no. 5, p. 2293–2304, 2017.
- [26] Y. Murakami and K. J. Miller, "What is fatigue damage? a viewpoint from the observation of low cycle fatigue process," *International Journal of Fatigue*, vol. 27, no. 10-12, pp. 991–1005, 2005.
- [27] G. Bebis *et al.*, "Feed-forward neural networks," *IEEE Potentials*, vol. 13, no. 5, pp. 27–31, Oct.-Nov. 1994.

- [28] M. H. Sazli, "A brief review of feed-forward neural networks," *Communications Faculty of Sciences University of Ankara Series A2-A3*, vol. 50, no. 1, pp. 11–17, 2006.
- [29] D. B. Barker and A. Dasgupta, "Thermal stress issues in plated-through-hole reliability," in *Thermal Stress and Strain in Microelectronics Packaging*, J. H. Lau, Ed. Van Nostrand Reinhold, 1993, pp. 648–682.
- [30] A. Navid *et al.*, "Diesel engine optimization with multi-objective performance characteristics by non-evolutionary nelder-mead algorithm: Sobol sequence and latin hypercube sampling methods comparison in doe process," *Fuel*, vol. 228, pp. 349–367, 2018.
- [31] A. M. J. Olsson *et al.*, "Latin hypercube sampling for stochastic finite element analysis," *Journal of Engineering Mechanics*, vol. 128, no. 1, pp. 121–125, 2002.
- [32] G. Joshi *et al.*, "Crack initiation and growth from pre-corroded pits in aluminum 7075-t6 under laboratory air and salt water environments," *Journal of Materials Engineering and Performance*, vol. 26, no. 5, pp. 2293–2304, 2017.
- [33] R. Seifi *et al.*, "Experimental study of fatigue crack growth in raw and annealed pure copper with considering cyclic plastic effects," *[Journal Name]*, vol. [Volume], p. [Pages], 2018.
- [34] S. Golestan *et al.*, "Moving average filter based phase-locked loops: Performance analysis and design guidelines," *IEEE Transactions on Power Electronics*, vol. 29, no. 6, pp. 2750–2763, June 2014.
- [35] T. van Erven and P. Harremoës, "Rényi divergence and kullback-leibler divergence," *IEEE Transactions on Information Theory*, vol. 60, no. 7, pp. 3797–3820, July 2014.